Spatial Chemical Inhomogeneity and Local Electronic Structure of Mn-Doped Ge Ferromagnetic Semiconductors

J.-S. Kang,[1,*] G. Kim,[1] S. C. Wi,[1] S. S. Lee,[1] S. Choi,[2] Sunglae Cho,[2] S. W. Han,[3] K. H. Kim,[3] H. J. Song,[4] H. J. Shin,[4] A. Sekiyama,[5] S. Kasai,[5] S. Suga,[5] and B. I. Min[6]

[1]*Department of Physics, The Catholic University of Korea, Puchon 420-743, Korea*
[2]*Department of Physics, University of Ulsan, Ulsan 680-749, Korea*
[3]*Department of Physics, Gyeongsang National University, Chinju 660-701, Korea*
[4]*Pohang Accelerator Laboratory (PAL), POSTECH, Pohang 790-784, Korea*
[5]*Department of Material Physics, Graduate School of Engineering Science, Osaka University, Osaka 560-8531, Japan*
[6]*Department of Physics, POSTECH, Pohang 790-784, Korea*

(Received 2 September 2004; published 11 April 2005)

We have investigated the chemical distributions and the local electronic structure of potential diluted magnetic semiconductor $Ge_{0.94}Mn_{0.06}$ single crystals using scanning photoelectron microscopy (SPEM), x-ray absorption spectroscopy (XAS), and photoemission spectroscopy (PES). The SPEM image shows the stripe-shaped microstructures, which arise from the chemical phase separation between the Mn-rich and Mn-depleted phases. The Mn $2p$ XAS shows that the Mn ions in the Mn-rich region are in the divalent high-spin Mn^{2+} states but that they do not form metallic Mn clusters. The Mn $3d$ PES spectrum exhibits a peak centered at $\sim$4 eV below E_F and the negligible spectral weight near E_F. This study suggests that the observed ferromagnetism in $Ge_{1-x}Mn_x$ arises from the phase-separated Mn-rich phase.

DOI: 10.1103/PhysRevLett.94.147202 PACS numbers: 75.50.Pp, 68.37.Xy, 79.60.-i

One promising strategy to achieve spin injection into nonmagnetic semiconductors in spintronics is to use a diluted magnetic semiconductor (DMS), prepared by substituting $3d$ transition-metal (TM) ions, such as Cr, Mn, Fe, Co, and Ni, into nonmagnetic semiconductors. Interest in DMS materials has been reinvoked with the discovery of spontaneous ferromagnetic (FM) order in $Ga_{1-x}Mn_xAs$ [1] exhibiting the Curie temperature T_C up to 110 K. Theoretically, mean-field calculations of a Zener model [2] predicted that the FM order can be stabilized in Mn-doped semiconductors with sufficiently high hole carriers. Recent experiments show that both Ge films [3,4] and bulk single crystals [5] doped with Mn ions exhibit the FM ordering at $T_C \sim 116$ K and at $T_C \sim 285$ K, respectively. Also the FM ordering at $T_C \sim 270$ K was reported for Co and Mn-doped Ge epitaxial films [6].

The origin of the ferromagnetism in DMSs is still controversial, and the reproducibility of the FM order in DMSs is questionable, as found in contradicting reports on $Zn_{1-x}Co_xO$ [7–9] and anatase $Ti_{1-x}Co_xO_2$ [10]. One of the key issues in this field is whether there is no phase separation of dopants in DMSs. Therefore it is very important to investigate the possibility of the phase separations in DMSs in the micrometer (μm) or nanometer scale, and to investigate the electronic structures of doped TM impurities. In this aspect, scanning photoelectron microscopy (SPEM) is a powerful method for studying the chemical distribution of dopant elements in sub-μm scale [11]. In SPEM, x rays are focused through a focusing lens (or a zone plate) to a sub-μm scale spot. By scanning a sample at a characteristic photon energy $h\nu$ corresponding to a certain element, one can obtain the spectral image for the chemical distribution of that element [11]. No SPEM study on DMS materials has been reported so far. On the other hand, photoemission spectroscopy (PES) and x-ray absorption spectroscopy (XAS) are the essential experimental tools for providing direct information on the electronic structures and the valence states of TM ions in solids [12,13]. Only a few experimental PES/XAS studies have been reported on potential DMS materials [14–17], but not on $Ge_{1-x}Mn_x$.

In this Letter, we have investigated the sub-μm scale chemical distribution and the electronic structure of $Ge_{0.94}Mn_{0.06}$ single crystals by combining SPEM, XAS, and PES methods in order to understand the nature and the origin of ferromagnetism in Mn-doped Ge. Single-crystalline $Ge_{1-x}Mn_x$ samples were made by using high-purity (99.999%) Ge and Mn powders of the particle size less than -200 mesh. The details of the sample preparation and characterization are described in Ref. [5]. In the x-ray diffraction (XRD) analysis of these samples, no impurity phases were detected within the experimental detection limit. Caution is needed, however, since the presence of nanoscale impurity phases within the host matrix cannot be completely excluded by the standard XRD technique. The Laue diffraction patterns showed that these samples were single crystals with diamond structures, and the lattice constant increased linearly with increasing Mn concentration. Both results indicate that Mn ions were substituted properly for the host Ge sites. These crystals exhibited the paramagnetic to FM transition at $T_C \sim 285$ K and the FM to antiferromagnetic transition at $T_C \sim 150$ K (see Fig. 3 in Ref. [5]).

SPEM, PES, and XAS measurements were performed at the 8A1 undulator beam line of the Pohang Accelerator Laboratory. A 50 μm pinhole is placed between the zone

plate and the sample, resulting in the size of the focused x rays on the sample to be about 0.5 μm in diameter [11]. Topographic SPEM images are constructed either by the total intensity over 16 channels in the photoelectron detector arrays or by employing the total electron yield method (sample current). The latter method is known to be more bulk representative owing to the longer probing depth. Before samples were introduced into the SPEM chamber, they were polished by using the abrasive papers and diamond powders up to 1 μm in size. The SPEM images were obtained first from the as-is surfaces. Then samples were sputtered mildly with Ne ions to remove carbons (C) on sample surfaces but to minimize the possible artifacts caused by sputtering. All the measurements were done at room temperature, and with the pressure better than 4×10^{-10} Torr. All the spectra were normalized to the incident photon flux. XAS spectra were obtained by employing the total electron yield method, with the photon energy resolution of $\sim$100 meV at the Mn $2p$ absorption threshold ($h\nu \approx 640$ eV).

Mn $2p \rightarrow 3d$ resonant PES (RPES) experiments were performed at the twin-helical undulator beam line BL25SU of SPring-8 equipped with a SCIENTA SES200 analyzer. Samples were fractured and measured in vacuum better than 3×10^{-10} Torr at $T \lesssim 20$ K. The Fermi level E_F and the FWHM of the system were determined from the valence-band spectrum of a scraped Pd in electrical contact with samples. PES data were obtained in the transmission mode, with the FWHM of about 100 meV at $h\nu \sim 600$ eV. All the spectra were normalized to the photon flux.

The top left of Fig. 1 shows the SPEM image of $Ge_{0.94}Mn_{0.06}$. The scan area and the step size of this SPEM image were 1000 μm $\times$ 1000 μm and 20 μm $\times$ 20 μm, respectively. In obtaining the SPEM image, the photon energy was set at the Mn $2p_{3/2}$ absorption peak ($h\nu \approx 640$ eV, see Fig. 3), and SPEM images were constructed by employing the total electron yield method. Thus this SPEM image represents the chemical distributions of Mn ions, and the brightness is proportional to the relative Mn concentration. Further, this SPEM image can be considered to represent the bulk features of the measured samples [18]. The SPEM image reveals the stripe-shaped bright regions with a width of a few tens μm and a length of a few hundreds μm. The bright (B) and dark (D) spots in the image correspond to the Mn-rich and Mn-depleted region, respectively, as confirmed in the survey PES spectra on the right.

The top right of Fig. 1 shows the survey PES spectra of $Ge_{0.94}Mn_{0.06}$, obtained at the bright (B) spot and the dark (D) spot, respectively, and with $h\nu \approx 640$ eV. The survey spectrum for a dark spot is essentially the same as that for pure Ge, indicating that the average Mn concentration in the dark region is very low. In contrast, the survey spectrum for a bright spot reveals the large Mn-derived features, such as the Mn $3d$ peak and Mn LMM Auger peaks. Therefore these survey PES spectra provide evidence that the bright (B) and dark (D) regions in the SPEM image correspond to

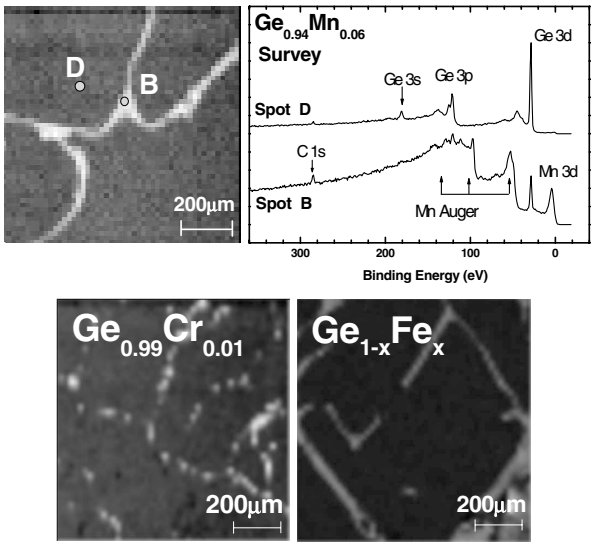

FIG. 1. Top: The SPEM image (left) and the survey spectra (right) of $Ge_{0.94}Mn_{0.06}$, obtained at a bright spot (B) and a dark spot (D). Bottom: SPEM images of $Ge_{0.99}Cr_{0.01}$ and $Ge_{1-x}Fe_x$ ($x \approx 0.05$).

the Mn-rich and Mn-depleted phases, respectively. We note that the magnetic properties of $Ge_{0.94}Mn_{0.06}$ [5] are similar to those of Ge_8Mn_{11} (see Fig. 1 in Ref. [19]). It is thus likely that the Mn-rich phase in $Ge_{0.94}Mn_{0.06}$ actually consists of several Ge_xMn_y alloys, including Ge_8Mn_{11} [19,20]. This finding suggests that preparing homogeneous $Ge_{1-x}Mn_x$ DMS samples is very difficult. This may be the reason why very few works have been reported on the $Ge_{1-x}Mn_x$ system so far, either bulk [5] or films [3,4]. By comparing the magnetization data between our $Ge_{0.94}Mn_{0.06}$ crystal [5] and Ge_8Mn_{11} [19], we have roughly estimated the volume fraction of the impurity phase of $\sim$2% in our sample, which implies that some of the doped Mn ions form Mn-rich alloys, and the rest of them are substituted for the Ge sites.

The bottom of Fig. 1 shows the SPEM images of $Ge_{0.99}Cr_{0.01}$ and $Ge_{1-x}Fe_x$ ($x \approx 0.05$) [21], which were obtained at the Cr and Fe $2p_{3/2}$ absorption peaks, respectively, and constructed from the total electron yields. These images also exhibit the stripe-shaped bright regions. The survey spectra show [22] that the bright and dark regions in the SPEM images correspond to the Cr(Fe)-rich and Cr(Fe)-depleted phases. Therefore these observations provide evidence that $Ge_{1-x}T_x$ (T = Cr, Mn, Fe) crystals consist of the microstructures with very different T concentrations.

Figure 2 compares the Mn $2p$ XAS spectrum of $Ge_{0.94}Mn_{0.06}$ to those of reference Mn compounds having formal Mn valences of 2+ (MnS [23], MnO [24]) and 4+ (MnO_2 [24]), and that of Mn metal [25]. The peak positions and the line shape of the Mn $2p$ XAS spectrum depend on the local electronic structure of the Mn ion, and provide the information on the valence state and the ground-state symmetry of the Mn ion [12,13]. The Mn $2p$ XAS spectrum of

$Ge_{0.94}Mn_{0.06}$ looks similar to those of MnS and MnO, except for the absence of the low-$h\nu$ shoulder ($h\nu \sim 639$ eV), but quite different from those of MnO_2 and Mn metal. This observation suggests that the valence states of Mn ions in $Ge_{0.94}Mn_{0.06}$ are nearly divalent (Mn^{2+}) but not tetravalent (Mn^{4+}), and that the formation of the Mn metal cluster in our $Ge_{0.94}Mn_{0.06}$ samples is ruled out.

In order to confirm this effect, we have included the calculated Mn $2p$ XAS spectrum for a Mn^{2+} ($3d^5$) ion in the tetrahedral (T_d) symmetry (reproduced from Ref. [13]) at the bottom of Fig. 2. The calculation is based on the cluster model which includes the effects of the multiplet interaction, the crystal field, and the hybridization with the ligand orbitals. The Mn^{2+} ($3d^5$) configuration and the small T_d crystal field energy of $10Dq = 0.5$ eV yields a good fit for the measured Mn $2p$ XAS spectrum of $Ge_{0.94}Mn_{0.06}$. The small value of $10Dq = 0.5$ eV implies that Mn ions are in the high-spin (HS) states. The similarity between the measured Mn $2p$ XAS spectrum and the calculated $2p$ XAS spectrum indicates that the doped-Mn ions in $Ge_{0.94}Mn_{0.06}$ are in the HS divalent Mn^{2+} (d^5) states with the total spin of $S = 5/2$. This analysis also reveals [13] that the line shapes of the XAS spectra for small $10Dq$ are very similar between the O_h (octahedral) and T_d symmetries.

Figure 3 shows the valence-band RPES spectra of $Ge_{0.94}Mn_{0.06}$ near the Mn $2p_{3/2}$ absorption edge, obtained at $T \lesssim 20$ K. The inset shows the corresponding Mn $2p_{3/2}$ XAS spectrum of $Ge_{0.94}Mn_{0.06}$. The off-resonance valence-band PES spectrum (A) is similar to the valence-band x-ray photoemission spectroscopy spectrum for pure Ge [26], as expected from the small average Mn concentration ($\sim$6%) in $Ge_{1-x}Mn_x$ in addition to the smaller photoionization cross sections of Mn $3d$ electrons (by an order of magnitude) than those of Ge $3d$ electrons. Then the enhanced features near $\sim$4 eV binding energy at the Mn $2p \rightarrow 3d$ absorption energy (C) represent the resonating Mn $3d$ electron emission. Therefore the difference between the on-resonance and off-resonance spectra can be considered to represent the *bulk* Mn $3d$ partial spectral weight (PSW) distribution [27].

Figure 4 presents the extraction procedure of the Mn $3d$ PSW for $Ge_{0.94}Mn_{0.06}$. As a first approximation, it is taken as the difference (dotted line) between the Mn $2p \rightarrow 3d$ on-resonance spectrum (solid line) and off-resonance spectrum (gray line). The extracted Mn $3d$ PSW exhibits a peak centered at $\sim$4 eV binding energy with the FWHM of $\sim$4 eV and a weak tail to the high binding energy side (up to $\sim$12 eV). The Mn $3d$ PSW for $Ge_{0.94}Mn_{0.06}$ shows that Mn $3d$ states are located well below E_F, indicating that the doped-Mn $3d$ electrons occupy the very deep levels.

The extracted Mn $3d$ PSW of $Ge_{0.94}Mn_{0.06}$ is compared to that of $Ga_{0.931}Mn_{0.069}As$ film (Ref. [15]) at the bottom of Fig. 4. The position of the main peak for $Ge_{0.94}Mn_{0.06}$ is the same as that for $Ga_{0.931}Mn_{0.069}As$. However, the spectral weight between E_F and $\sim$2 eV binding energy is negligible in the $Ge_{0.94}Mn_{0.06}$ crystal, but clearly observable in the $Ga_{0.931}Mn_{0.069}As$ film [28]. In the cluster model analysis [15], the Mn $3d$ PSW for $Ga_{1-x}Mn_xAs$ was interpreted to represent the Mn^{2+} valence state, and the spectral weight between E_F and $\sim$2 eV binding energy arose mainly from the $d^5\underline{L}^1$ final-state component ($\underline{L}$: a ligand hole). Similarly, our Mn $3d$ PSW for $Ge_{0.94}Mn_{0.06}$ can be interpreted to represent the Mn^{2+} valence state, but to have the negligible $d^5\underline{L}^1$ final-state component. The presence of the $d^5\underline{L}^1$ final-state component in PES of Mn-doped GaAs film occurs when there is charge transfer from neighboring

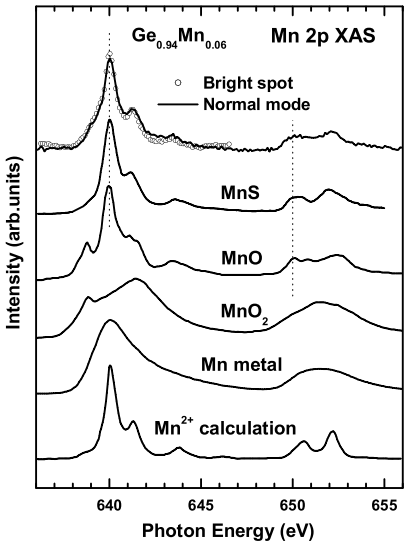

FIG. 2. Comparison of the Mn $2p$ XAS spectrum of $Ge_{0.94}Mn_{0.06}$ to those of MnS (Mn^{2+}) (Ref. [23]), MnO (Mn^{2+}) (Ref. [24]), MnO_2 (Co^{3+}) (Ref. [24]), and Mn metal (Ref. [25]). At the bottom is shown the calculated Mn $2p$ XAS spectrum for a $Mn^{2+}(3d^5)$ ion (Ref. [13]).

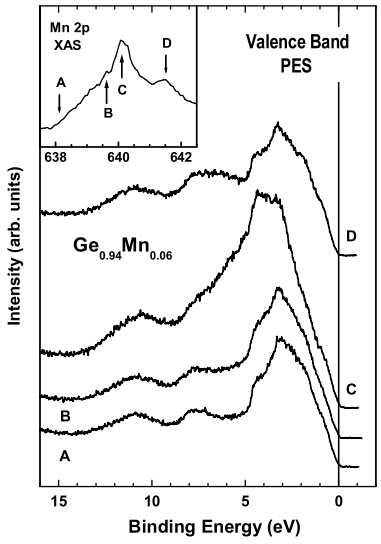

FIG. 3. Valence-band PES spectra of $Ge_{0.94}Mn_{0.06}$ near the Mn $2p_{3/2} \rightarrow 3d$ absorption edge. Inset: The Mn $2p_{3/2}$ XAS spectrum of $Ge_{0.94}Mn_{0.06}$. Arrows denote $h\nu$'s where the valence-band PES spectra were obtained.

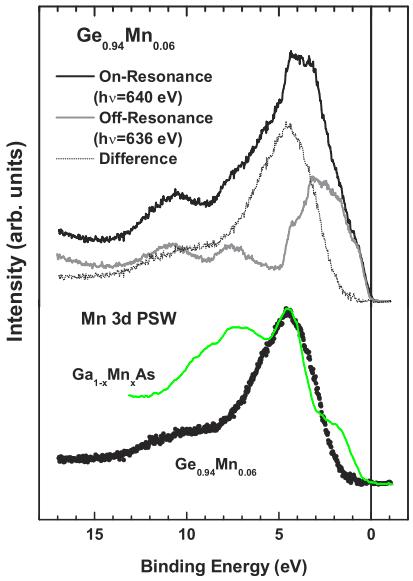

FIG. 4 (color online). Top: Comparison of the on-resonance (solid line) and off-resonance valence-band spectra (gray line) in Mn $2p \rightarrow 3d$ RPES. The difference curve between two spectra is shown as a dotted line. Bottom: Comparison of the extracted Mn $3d$ PSW of $Ge_{0.94}Mn_{0.06}$ to that of $Ga_{0.931}Mn_{0.069}As$ (Ref. [15]).

As $4p$ electrons to Mn $3d$ electrons, which requires substantially large hybridization between Mn $3d$ and As $4p$ states. Therefore the negligible $d^5\underline{L}^1$ final-state component in $Ge_{0.94}Mn_{0.06}$ suggests that the hybridization between Mn $3d$ and Ge $4p$ orbitals is much weaker than that between Mn $3d$ and As $4p$ states in $Ga_{0.931}Mn_{0.069}As$. Finally, the Mn $3d$ PSW with the main peak at $\sim$4 eV is quite different from the Mn $3d$ partial density of states of the local density approximation (LDA) band results for Mn-doped Ge [29,30], which exhibit the Mn $3d$ peaks at $\sim$2 eV. One can attribute this difference to the Coulomb correlation effect between Mn $3d$ electrons, which is not properly described in the LDA scheme. In fact, the LDA + U calculation for Mn-doped GaAs, incorporating the Coulomb interaction $U = 4.0$ eV, yields the peak position in agreement with that of the Mn $3d$ PSW, reflecting the importance of Mn $3d$ correlation effects [31].

In conclusion, the present study by using SPEM, XAS, and PES indicates that the $Ge_{0.94}Mn_{0.06}$ crystal is chemically phase separated into the Mn-rich and Mn-depleted phases. The stripe-shaped bright regions are observed in the SPEM images of $Ge_{0.94}Mn_{0.06}$ crystals, reflecting the inhomogeneous distribution of Mn concentrations. The simultaneous PES measurements provide evidence that the bright and dark regions in the SPEM images correspond to the Mn-rich and Mn-depleted phases, respectively. The Mn $2p$ XAS spectrum of $Ge_{0.94}Mn_{0.06}$ indicates that Mn ions are in the divalent states, but that they do not form pure metal clusters. This finding is consistent with the Mn $3d$ PSW, determined from Mn $2p \rightarrow 3d$ RPES. This study indicates that the ferromagnetism observed in $Ge_{1-x}Mn_x$ ($x \ll 1$) systems [3–5] may not be an intrinsic nature of DMSs, but arises from the magnetic properties of the Mn-rich phases in phase-separated $Ge_{1-x}Mn_x$.

We thank V. Kiryukhin for helpful discussions. This work was supported by the KRF (KRF-2002-070-C00038) and by the KOSEF through the CSCMR at SNU and the eSSC at POSTECH. The PAL is supported by the MOST and POSCO in Korea.

*Electronic address: kangjs@catholic.ac.kr

[1] H. Ohno *et al.*, Science **281**, 951 (1998).
[2] T. Dietl *et al.*, Science **287**, 1019 (2000).
[3] Y. D. Park *et al.*, Science **295**, 651 (2002).
[4] F. D'Orazio *et al.*, J. Magn. Magn. Mater. **272–276**, 2006 (2004).
[5] S. Cho *et al.*, Phys. Rev. B **66**, 033303 (2002).
[6] F. Tsui *et al.*, Phys. Rev. Lett. **91**, 177203 (2003).
[7] K. Ueda, H. Tabata, and T. Kawai, Appl. Phys. Lett. **79**, 988 (2001).
[8] J. H. Kim *et al.*, J. Appl. Phys. **92**, 6066 (2002).
[9] H. J. Lee *et al.*, Appl. Phys. Lett. **81**, 4020 (2002).
[10] J.-Y. Kim *et al.*, Phys. Rev. Lett. **90**, 017401 (2003).
[11] M. K. Lee and H. J. Shin, Rev. Sci. Instrum. **72**, 2605 (2001).
[12] F. M. F. de Groot *et al.*, Phys. Rev. B **42**, 5459 (1990).
[13] G. van der Laan and I. W. Kirkman, J. Phys. Condens. Matter **4**, 4189 (1992).
[14] T. Mizokawa *et al.*, Phys. Rev. B **65**, 085209 (2002).
[15] J. Okabayashi *et al.*, Phys. Rev. B **59**, R2486 (1999).
[16] Y. Ishiwata *et al.*, Phys. Rev. B **65**, 233201 (2002).
[17] S. C. Wi *et al.*, Appl. Phys. Lett. **84**, 4233 (2004).
[18] SPEM measurements were also done for the samples that were scraped *in situ*. We still observed the inhomogeneous regions, even though the images were not very clear due to the rough surfaces after scraping. This finding indicates that the observed inhomogeneous images are not due to the surface segregation nor due to the artifact caused by sputtering.
[19] N. Yamada *et al.*, J. Phys. Soc. Jpn. **55**, 3721 (1986).
[20] Y. D. Park *et al.*, Appl. Phys. Lett. **78**, 2739 (2001).
[21] S. Choi *et al.*, J. Appl. Phys. **93**, 7670 (2003).
[22] G. Kim *et al.* (unpublished).
[23] S. P. Cramer *et al.*, J. Am. Chem. Soc. **113**, 7937 (1991).
[24] C. Mitra *et al.*, Phys. Rev. B **67**, 92404 (2003).
[25] Y. Yonamoto *et al.*, Phys. Rev. B **63**, 214406 (2001).
[26] W. B. Jackson and J. W. Allen, Phys. Rev. B **37**, 4618 (1988).
[27] J.-S. Kang *et al.*, Phys. Rev. B **66**, 113105 (2002).
[28] The Mn $3d$ PSW for $Ga_{0.931}Mn_{0.069}As$ was determined by using the *surface-sensitive* Mn $3p \rightarrow 3d$ RPES technique, while our Mn $3d$ PSW for $Ge_{0.94}Mn_{0.06}$ is determined by using more *bulk-sensitive* Mn $2p \rightarrow 3d$ RPES (see Ref. [27]).
[29] Y.-J. Zhao, T. Shishidou, and A. J. Freeman, Phys. Rev. Lett. **90**, 047204 (2003).
[30] A. Stroppa *et al.*, Phys. Rev. B **68**, 155203 (2003).
[31] J. H. Park, S. K. Kwon, and B. I. Min, Physica (Amsterdam) **281B–282B**, 703 (2000).